Dynamic Ionic Strength Effects in Fast Bimolecular Electron Transfer between a Redox Metalloprotein of High Electrostatic Charge and an Inorganic Reaction Partner

Thomas J. Jensen,[†] Harry B. Gray,*[,‡] Jay R. Winkler,*[,‡] Alexander M. Kuznetsov,[§] and Jens Ulstrup*[,†]

Department of Chemistry, Building 207, Technical University of Denmark, DK-2800 Lyngby, Denmark, Beckman Institute, California Institute of Technology, Pasadena, California 91125, and A. N. Frumkin Institute of Electrochemistry of the Russian Academy of Sciences, Leninskij Prospect 31, 117071 Moscow, Russia

Received: April 27, 2000; In Final Form: September 28, 2000

The ionic strength dependence of the bimolecular electron transfer (ET) reaction between *Clostridium pasteurianum* rubredoxin(III) and photochemically generated $[Ru(bpy)_3]^+$ has been investigated. The reaction is fast and close to the diffusion-controlled limit. Dynamic ionic strength effects on all kinetics parameters (work terms, driving force, and reorganization free energy) have been incorporated in the data analysis; the effects on the intermolecular work terms are large and dominate in the driving force region close to the activationless limit. The variation in ET rate constant over the 0.005−2.0 M ionic strength range is quantitatively consistent with the high negative charge (−9*e* where *e* is the unit electric charge) and size (crystallographic radius ≈ 12 Å) of rubredoxin(III). If low ionic strength (0.005−0.01 M) data are omitted, the variation in rates suggests a somewhat smaller charge on the protein (−4*e* to −5*e*).

1. Introduction

Ionic strength effects on electron transfer (ET) reactions of redox metalloproteins can provide information about local surface charge and recognition patterns.[1−7] In most cases the ionic strength effects have been interpreted in terms of the Brønsted-Bjerrum[8−10] and Debye theories[11] of interionic interaction. Extension to planar charge distributions or models that go beyond the formal point charge constraints of Debye−Hückel theory have been introduced.[12] These models tend to focus on *static* ionic strength screening between the reaction partners that affects the interionic interaction or work terms for assembly of the reactant complex. Ionic strength variations also can perturb the Gibbs free-energy change for the reaction ($\Delta G°$) and the environmental reorganization Gibbs free energy (E_r).[13−15] The ionic strength dependence of $\Delta G°$ can be important for low-driving-force ET reactions and the reorganization energy for a reaction between ions of low charge can be quite sensitive to the ionic strength. Notably, the rates of ET reactions close to the activationless limit are weakly dependent on $\Delta G°$ and E_r so that ionic strength effects on these parameters can be neglected.

In this report we describe static and dynamic ionic strength effects on the ET reaction between the highly negatively charged (−9*e* where *e* is the unit electric charge) redox metalloprotein *Clostridium pasteurianum* rubredoxin(III) (rd(III)),[16−19] and photogenerated $[Ru(bpy)_3]^+$ (bpy = 2,2′-bipyridine), eq 1. This

$$\text{rd(III)} + [Ru(bpy)_3]^+ \rightarrow \text{rd(II)} + [Ru(bpy)_3]^{2+} \qquad (1)$$

pair of reactants offers significant advantages for studying electrostatic effects on intermolecular ET reactions of metalloproteins. The protein carries a large negative charge, particularly the region near the surface-exposed FeS_4 unit, the likely interaction site for the $[Ru(bpy)_3]^+$ ion. Since the highly exergonic reaction is nearly activationless, ET rates will be minimally affected by the ionic strength dependences of $\Delta G°$ and E_r. We have performed a detailed analysis of ionic strength effects on the ET kinetics of this reaction. Prior investigations of rd(III)/(II) ET have focused on the formal activation entropy,[20] pH effects,[21] self-exchange kinetics,[22] and reactions with flavins and protein-bound flavins.[23]

2. Materials and Methods

2.1. Reagents. Millipore water (Mille-Q-Housing) was used throughout. Tris buffer (tris-hydroxymethylaminomethane) and salts were Sigma reagent grade. $[Ru(bpy)_3]Cl_2$ was from Strem. *p*-Methoxydimethylaniline (*p*-MDMA) was synthesized and purified according to a standard procedure.[24]

Rubredoxin from *C. pasteurianum* was isolated and purified from a sample of engineered *Escherichia coli* (strain BL21-DE3, Novagen, kindly donated by M. K. Eidsness of the Center for Metalloenzyme Studies, University of Georgia) by a literature procedure.[19] A colony was stabbed with a toothpick and suspended in 2 mL of LB medium containing 100 mg/L of ampicillin. The solution was then incubated aerobically at 37 °C for 6 h, and 1 mL transferred to 50 mL of medium. After 12 h of incubation the cell suspension was divided into six 2 L flasks of medium, and incubated for 8 h. IPTC (isopropyl-β-D-thiogalactoside) was added to a concentration of 0.4 mM, inducing rd production. The cells were harvested by centrifugation 4 h later.

The cells were lysed by ultrasound (4 × 30 s), and the lysate diluted with 50 mM Tris buffer, pH 8. The cell material was removed by centrifugation (10 000 G, 30 min) and the lysate

[†] Technical University of Denmark.
[‡] California Institute of Technology.
[§] Russian Academy of Sciences.

10.1021/jp001624u CCC: $19.00
Published on Web 11/10/2000

loaded onto a QAE-Sephadex G-25 anion exchange column, and washed with 50 mM Tris, 150 mM NaCl, pH 8. The protein was then eluted with 0.5 M NaCl in the same buffer. The relevant fractions were isolated by ultrafiltration at 5 °C (3000 MW cutoff) and the buffer was changed to 50 mM Tris pH 8.5. This was followed by purification of the protein twice on a MonoQ column/Pharmacia FPLC system, using 50 mM Tris and 50 mM Tris, 1 M NaCl (both pH 8.5) as buffers A and B, respectively.

The concentration of rd(III) was determined by 490 and 380 nm absorbances ($\epsilon_{490} = 8.83 \times 10^3$ M^{-1} cm^{-1}, $\epsilon_{380} = 10.8 \times 10^3$ M^{-1} cm^{-1})[16] using a Hewlett-Packard 8452 diode array spectrophotometer. The absorbances of the resulting protein solution (0.50 at 380 nm and 0.43 at 490 nm relative to the absorption at 280 nm) were close to published values. The yield is 14 mg or 2.25 μmol. The protein was stored as concentrated solutions at −18 °C. The stock solutions did not freeze at this temperature. The only sign of deterioration was a tendency for the protein to precipitate, although it redissolved readily when warmed to room temperature.

2.2. Electrochemical Data. Rd was also characterized by cyclic voltammetry (CH Instruments, model 660 Electrochemical Workstation). The working electrode was edge plane pyrolytic graphite. A calomel reference electrode and a platinum wire counter electrode were used in a standard two-compartment cell. Voltammograms of a 0.7 mM rd(III) solution in 50 mM Tris buffer (pH 7.5) with 40 mM $MgSO_4$ as promoter were recorded. Reversible voltammograms were always obtained, with a midpoint potential of −60 mV (NHE), in agreement with the literature value.[25]

2.3. Transient Absorption Experiments. Solutions were made up in 10 mm cuvettes from stock solutions of rd (1.5−2.5 mM) and $[Ru(bpy)_3]Cl_2$ (1 mM), and diluted with buffer using Hamilton gastight glass syringes. MDMA (3 mg) was added in solid form. Rd stock solutions were diluted with buffer and concentrated by centrifugation in centricon tubes (3000 MW cutoff). Rd stock concentrations were determined by diluting a small sample of known volume and calculating the concentration on the basis of the absorbances at 490 and 380 nm. Samples were deoxygenated by repeated evacuation/Ar-fill cycles on a Schlenk line. This introduces some data variation as slightly uneven evaporation occurs. Decreases in volume were, however, less than 10%.

Reductive quenching was initiated by excitation of $[Ru(bpy)_3]Cl_2$ at 480 nm followed by reductive quenching by *p*-methoxy-dimethylaniline, according to eq 2.[26,27] A Lambda Physik FL

$$[Ru(bpy)_3]^{2+}* + MDMA \rightarrow [Ru(bpy)_3]^{+} + MDMA^{+} \quad (2)$$

3002 dye laser (Coumarin 480) pumped with a Lambda Physik LPX210i XeCl excimer laser (25 ns, 1−3 mJ) was the excitation source.[28] Single wavelength transients were recorded using a 75 W xenon arc lamp probe source propagating collinearly with the excitation source and passing through a double monochromator. The output was detected by a photomultiplier tube and amplified with a DSP 1402E programmable amplifier. Signals were digitized using a Tektronix RTD710 200 MS/s 10 bit transient digitizer interfaced to a PC.

Reactions were carried out at room temperature and followed at 350, 380, and 515 nm. The laser pulse interfered with the 490 nm band of rd(III) and the reaction could not be followed at this wavelength. $[Ru(bpy)_3]^{2+}*$ and *p*-$MDMA^+$ could be monitored at 515 nm,[26] confirming that quenching had taken place. The reduction of rd(III) was followed at 380 nm ($\Delta\epsilon_{380} \approx 10^4$ M^{-1} s^{-1}). Recorded transients are averages of at least 10

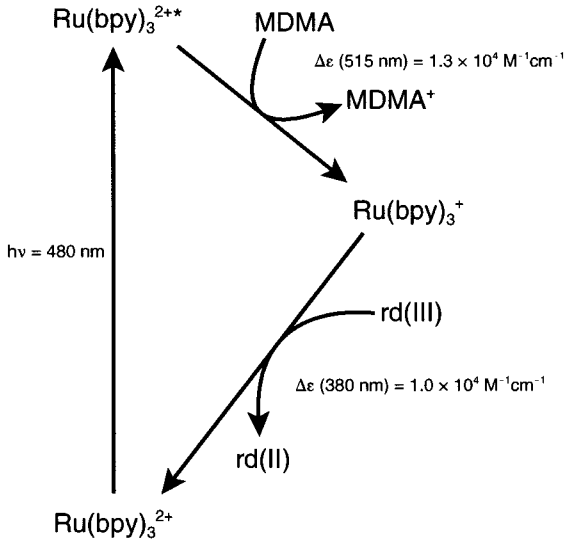

Figure 1. Reaction scheme for transient generation of $[Ru(bpy)_3]^+$ and subsequent ET with rd(III).

experiments. Solutions of 20, 40, 60, and 80 μM rd were measured at each ionic strength. This corresponds to a large excess of rd relative to transient $[Ru(bpy)_3]^+$. The data were fit to biexponential functions using a nonlinear least-squares algorithm; the rate constant for the faster phase was 1−2 orders of magnitude greater than that of the slower phase. The fast phase corresponds to ET between $[Ru(bpy)_3]^{2+}*$ and *p*-MDMA ($[Ru(bpy)_3]^{2+}*$ has measurable absorbance at 380 nm), the slow phase to the reduction of rd(III) by $[Ru(bpy)_3]^+$. The rate constant for the fast phase was only weakly dependent on [rd(III)], whereas the slow-phase rate constant varied linearly with [rd(III)] at all ionic strengths. Higher rd concentrations were examined at $I = 0.1$ M to test for saturation kinetics (although signal/noise was problematic at the highest concentrations). The finite intercept and initial nonlinearity at the lowest ionic strength (0.005 M) could indicate that there is another reaction channel.

3. Results and Discussion

3.1. Rate Constants. Figure 1 shows the reaction scheme. $[Ru(bpy)_3]^{2+}*$, prepared by laser excitation at 480 nm, is reduced by *p*-methoxy-dimethylaniline. The reduction product, $[Ru(bpy)_3]^+$, then reduces rd(III), eq 1. Figure 2 shows the transient absorption of rd(III) at 380 nm. The decay follows first-order kinetics, with pseudo-first-order rate constants linear in the rd(III) concentration in the range 5−100 μM (Figure 3).

Rate constants were recorded over the range of ionic strengths, *I*, from 5 mM to 2.0 M (Figure 4). The ionic strength is related to the inverse Debye length, according to eq 3, where

$$\kappa = \sqrt{\frac{8\pi e^2 I}{\epsilon_s k_B T}} \quad (3)$$

ϵ_s is the static dielectric constant of water (78), k_B is Boltzmann's constant, and *T* is temperature. The second-order rate constants are large and close to the diffusion limit. As expected from the high negative charge of rd(III) (−9*e*), the reaction slows significantly with increasing ionic strength; the rate constant decreases by almost an order of magnitude for *I* ranging from 5 mM to 2.0 M.

3.2. Static and Dynamic Ionic Strength Effects. The data can be interpreted in terms of ET theory; but this requires consideration of the principal dynamic character of ionic strength

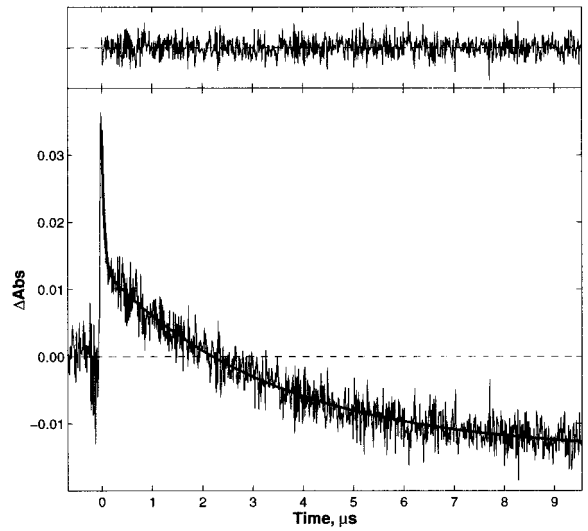

Figure 2. Transient absorption at 380 nm following excitation of $[Ru(bpy)_3]^{2+}$ at 480 nm in the presence of MDMA and rd(III) ([rd(III)] = 60 μM; I 0.1 M; Tris buffer, pH 7). The fast decay phase corresponds to loss of $[Ru(bpy)_3]^{2+*}$; the slower phase is due to reaction of $[Ru(bpy)_3]^{+}$. The solid line is a biexponential fit to the data and the upper panel shows the residuals.

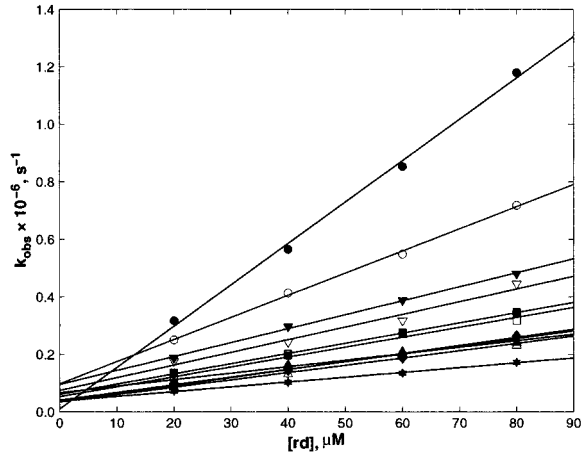

Figure 3. Observed first-order rate constants as a function of [rd(III)] for different ionic strengths (Tris buffer, pH 7.0): (●) I 0.005 M; (○) 0.01; (▼) 0.05; (▽) 0.07; (■) 0.10; (□) 0.20; (◆) 0.35; (◇) 0.50; (▲) 0.70; (△) 1.00; (★) 2.00.

effects as well as possible effects of partial diffusion control. When diffusion control is unimportant, the observed bimolecular ET rate constant ($M^{-1}s^{-1}$) is[29,30]

$$k_{ET}^{(2)} = \Delta V k_{ET}^{(1)} \qquad k_{ET}^{(1)} = \nu_{el}\frac{\omega_{eff}}{2\pi}\exp\left[-\frac{G^{\ddagger}}{k_B T}\right] \tag{4}$$

$$G^{\ddagger} = w_R + \frac{(E_{rs} + E_{r\kappa} + \Delta G^0 + w_P - w_R)^2}{4(E_{rs} + E_{r\kappa})} \tag{5}$$

where $k_{ET}^{(1)}$ (s^{-1}) is the transition probability per unit time for ET between the donor and acceptor in a "collision complex" and ΔV is the volume of the reaction zone for bimolecular ET. The first of eqs 4 provides the relationship between the observed bimolecular rate constant, $k_{ET}^{(2)}$, and the (quantum mechanical) transition probability, $k_{ET}^{(1)}$. The activation free energy, $G^{\ddagger}$, includes contributions from the reaction free-energy change, $\Delta G°$, the intermolecular work terms in the reactant, w_R, and

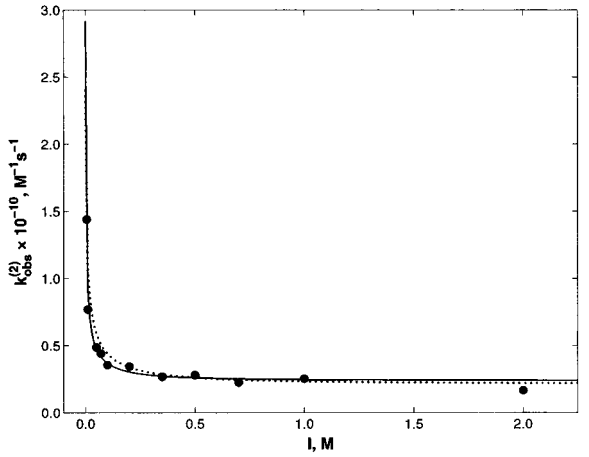

Figure 4. Ionic strength dependence of the rd(III) + $[Ru(bpy)_3]^{+}$ second-order ET rate constants (Tris buffer, pH 7.0). Solid line was calculated assuming reaction control (eqs 9 and 13: a_A = 13.7 Å; z_A = −7.4e); dotted line was calculated assuming partial diffusion control (eqs 10−13: a_A = 7.4 Å; z_A = −5.7e).

product states, w_P, the solvent reorganization free energy, E_{rs}, and the reorganization free energy of the ionic atmosphere, $E_{r\kappa}$. Intramolecular reorganization is disregarded, ν_{el} is the electronic transmission coefficient, and ω_{eff} is the effective vibrational frequency of all the classical nuclear modes.

When the reaction is partially diffusion-controlled, the observed bimolecular ET rate constant is given by eq 6 (Appendix), where $\vec{k}_{diff}^{(2)}$ ($M^{-1}s^{-1}$) is the bimolecular rate constant for

$$k_{obs}^{(2)} \approx \frac{k_{ET}^{(1)}\vec{k}_{diff}^{(2)}}{k_{ET}^{(1)} + \overleftarrow{k}_{diff}^{(1)}} \tag{6}$$

forward diffusion to form the collision complex where ET occurs and $\overleftarrow{k}_{diff}^{(1)}$ (s^{-1}) is the formally unimolecular rate constant for the reverse of this process. Specific forms of these rate constants are addressed below and in the Appendix.

The dominant ionic strength effects are associated with the work terms. These include all interactions between the reacting molecules, screened by the solvent and the ionic atmosphere. Ionic strength effects are also reflected in the driving force, $-\Delta G°$, via the activity coefficients of the reactant and product molecules. Finally, owing to *dynamic* reorganization of the ionic atmosphere, these effects produce a Franck−Condon barrier, reflected in the reorganization energy, $E_{r\kappa}$. By comparison, the ionic strength dependence in the preexponential factors is small and will be neglected. We offer the following:

(1) Ionic strength effects in the Brønsted-Bjerrum or Debye−Hückel formalism focus solely on w_R in eq 5. This term often *dominates* (see below) but significant effects can also arise from the ionic strength dependence of $\Delta G°$ and the combination $w_P - w_R$.

(2) Ionic strength effects on $\Delta G°$ correspond to the notion of "secondary" ionic strength effects[31] in the Brønsted-Bjerrum frame.

(3) Ion pair formation is not directly inherent in eqs 5 and 6 but can be incorporated if necessary.[30,32]

The reaction, eq 1, has a high driving force, $-\Delta G° \approx 1.2$ eV,[27] and is therefore close to the activationless limit. This simplifies the ionic strength dependence but also calls attention to partial diffusion control. These two features are addressed in the Appendix. Simplification of the ionic strength dependence can be achieved by recasting eq 5 in the following form,[13]

$$G^{\ddagger} = w_R^s + w_R^\kappa + \theta(\Delta G_s^0 + \Delta G_\kappa^0) + \theta(1-\theta)(E_{rs} + E_{r\kappa}) \quad (7)$$

where the index "s" refers to the pure solvent at zero ionic strength and "κ" to effects caused by the ionic atmosphere. θ is the chemical transfer coefficient, eq 8, and represents the degree

$$\theta = dG^{\ddagger}/d\Delta G^0 \qquad \theta = \frac{1}{2} + \frac{\Delta G^0}{2(E_{rs} + E_{r\kappa})} \quad (8)$$

of solvent and ionic strength reorganization on transfer from the equilibrium configuration of the reactants to the transition state. θ is close to 0.5 for low-driving-force reactions but approaches zero at the activationless limit. The first simplification is, then, that the ionic strength dependences of the driving force and the reorganization free energy are scaled by a small factor, $\theta \rightarrow 0$. The second simplification follows from the high charge of rd(III) ($-9e$). From the explicit ionic strength dependence of all the quantities in eq 7 (Appendix), it is apparent that the ionic strength dependence at *high* reactant charges is far stronger for w_R^κ than for the other quantities.

In the limit where diffusion is unimportant, the κ dependence of the rate constant can be recast in the form given by eq 9, where the superscripts on k_{ET} refer to the ionic strengths $\kappa \neq 0$ and $\kappa = 0$, respectively.

$$\ln\left(\frac{k_{ET}^{(2)\kappa}}{k_{ET}^{(2)\kappa=0}}\right) = -\frac{w_R^\kappa}{k_B T} \quad (9)$$

The second-order rate constants are in the range $\approx 10^{10}$ M^{-1} s^{-1} and close to the diffusion limit. These values accord with eq 4 and modify the ionic strength dependence of the observed rate constants. The ionic strength and reactant charge dependence of $\vec{k}_{diff}$ is described *approximately* by eq 10,[33,34] where

$$\vec{k}_{diff}^{(2)} = \vec{k}_{diff}^{(2)0}\frac{w_R}{k_B T}\frac{1}{\left[\exp\left(\frac{w_R}{k_B T}\right) - 1\right]} \qquad w_R = w_R^s + w_R^\kappa \quad (10)$$

$\vec{k}_{diff}^{(2)0}$ is the diffusion-controlled bimolecular rate constant for electrically *neutral* reactants and w_R^s is the inter-reactant interaction screened solely by the solvent (eq 11).

$$w_R^s = \frac{z_D z_A e^2}{\epsilon_s R} \quad (11)$$

It is shown further in the Appendix that

$$\frac{\vec{k}_{diff}^{(2)}}{\vec{k}_{diff}^{(1)}} = \Delta V \exp\left(-\frac{w_R}{k_B T}\right) \qquad w_R = w_R^s + w_R^k \quad (12)$$

where ΔV is the volume of the reaction zone introduced in eq 4. Equations 4−6 and 9−12 represent the observed, partially diffusion-controlled, second-order rate constant, with ionic strength dependences inherent in *both* k_{ET} and $\vec{k}_{diff}^{(2)}$.

No assumptions about the ionic strength dependence of interionic interactions have been invoked for the derivation of eqs 4−12. We shall employ explicitly the Debye interpolation formula[11] (eq 13) in the analysis of ET rates.

$$w_R^\kappa = \frac{z_D z_A e^2}{2\epsilon_s R}\left\{\frac{\exp[\kappa(a_D - R)]}{1 + \kappa a_D} + \frac{\exp[\kappa(a_A - R)]}{1 + \kappa a_A} - 2\right\} \quad (13)$$

In this expression, $z_D e$ and $z_A e$ are the charges of the donor and acceptor, respectively, a_D and a_A are the ionic radii, and R ($=a_D + a_A$) is the interionic distance.

Equations 9 and 13 have often been used in the analysis of ET kinetics, but they are not valid equations under all circumstances. To minimize the consequences of the ionic strength dependences of $\Delta G°$ and E_r, the reactants should be highly charged or the reactions close to the activationless limit. Equation 13 is an interpolation and applies rigorously only when $a_D = a_A$.[11] Finally, the Debye formula is based on the Debye−Hückel potential, which applies to spherically symmetric charge distributions. Globular metalloproteins, of course, only approximate this model when they are separated by distances comparable to their radii. Dielectric models in which the protein is treated as a local region of low dielectric constant, however, permit either exact[35] or numerical[36] determination of the electrostatic surface potential. Models of this type suggest that the protein surface charges oriented toward the incoming reaction partner, along with internal charges, contribute to the electrostatic potential approximately as similarly spaced charges free in solution. Surface charges on the opposite side of the protein are screened and contribute less to the work terms. The Debye formula (eq 13) is expected to provide a reasonably accurate description of the reaction between rd(III) and $[Ru(bpy)_3]^+$.

3.3. Ionic Strength Dependence of rd(III)/$[Ru(bpy)_3]^+$ ET. The data were compared with the theoretical ET rate constants both in the limits of pure reaction control (eqs 4, 5, 9, and 13) and when diffusion control is important (eqs 6 and 9−13). Good fits to the data were obtained in both cases. Figure 4 shows the best fit of eqs 9 and 13 to all the data; parameters were the apparent radius and charge of the protein (a_A, z_A). A radius of 7 Å and unit positive charge were taken for $[Ru(bpy)_3]^+$. The best values of a_A and z_A were 13.7 ± 5.5 Å and $-(7.4 \pm 3.3)e$. The former can be compared to the crystallographic radius determined previously;[1] and the latter is in accord with estimates of the total charge from the amino acid composition of the protein. If data for the two lowest ionic strengths are omitted, the variation of the rate constants appears significantly weaker, and lower charges are obtained. Smaller values of the apparent charge are, naturally, obtained if the protein radius is fixed at lower values. These modifications would simulate local surface structural elements. Radii fixed at 2 and 6 Å give, for example, rd(III) charges of $-1.6e$ and $-3.3e$, respectively. Fitting to the partially diffusion-controlled limit, eqs 4 and 10−13, included the additional parameter, $\vec{k}_{diff}^{(2)0}$. Values in the range $(2-5) \times 10^{10}$ M^{-1} s^{-1} were selected and the radius and charge of rd(III) left as free parameters. Unique values of these could not be determined but radii of 7.4 ± 3.4 Å and charges of $-(5.7 \pm 1.7)e$ were compatible with the data. High charges emerge in this limit as well, but the data do not permit us to discriminate between reaction control and partial diffusion control.

The apparent high negative charge of rd(III) estimated from the ionic strength dependence of the rate constants accords with the surface charge distribution of the protein. At least six negatively charged residues are grouped around the exposed FeS_4 complex in a hydrophobic surface region.[18] These residues would contact $[Ru(bpy)_3]^+$ as it approached the Fe−S cluster, which has a charge of $-e$ in the rd(III) state and $-2e$ in the rd(II) state. It is likely, then, that the high rd(III) surface charge at the $[Ru(bpy)_3]^+$ binding site is responsible for the ionic strength effects observed in this reaction.

In a previous investigation, a low apparent protein charge ($-e$) was extracted from analysis of the kinetics of reduction

of rd(III) by $[V(H_2O)_6]^{2+}$ at three ionic strengths in the range 0.01−0.1 M.[20] No details of the analysis were given but the pH values used (3.5−4.5) would accord with a lower apparent charge than that obtained in the present investigation. Our data are more suitably compared with ionic strength effects on the ET reactions between horse heart cytochrome *c* (cyt *c*) and the inorganic reaction partners $[Fe(EDTA)]^{2-}$, $[Fe(CN)_6]^{3-}$, and $[Co(phen)_3]^{3+}$ (phen = 1,10-phenanthroline).[1] Small apparent charges for cyt *c* ($\approx e$) were obtained when the data were analyzed in terms of the simplest Brønsted-Bjerrum relation, i.e., with reactant charges as the sole parameter. The data also were analyzed in terms of both Debye−Hückel theory combined with classical transition state theory, and in terms of the Debye relation in a form analogous to eq 13. In both cases the reactant radii were fixed and the cyt *c* charge left as the only parameter. First, this analysis showed that apparent charges are generally lower when transition state theory is used than when the Debye model is used. Second, as expected, apparent charges decrease when fixed radii are made smaller. Finally, the apparent protein charge shows some variation with the inorganic reaction partner, reflecting local charge effects. The apparent charges are, for example, quite close to the real charge ($+7e$) for the negatively charged inorganic reactants $[Fe(EDTA)]^{2-}$ ($+8.1e$) and $[Fe(CN)_6]^{3-}$ ($+6.6e$) when the crystallographic radius is chosen (16.6 Å). In comparison, a notably lower value ($+4.7e$) emerges for the positively charged reaction partner, $[Co(phen)_3]^{3+}$. The cyt *c* reactions, however, belong to the *normal* rather than the activationless free energy range. A more complete ionic strength analysis should therefore not rest solely on eq 13 but also incorporate eqs A6−A8 combined with eq 7. Further, the additional driving force effects represented by eqs A7 and A8 could be significant, owing in particular to the high charge of cyt *c*.

Appendix: Formulation of Dynamic Ionic Strength Effects

A.1. Bimolecular ET Rate Constant. To describe the ionic strength effect quantitatively, eq 5 can first be compared with the following form known from ET theory[30]

$$G^{\ddagger} = G^{\ddagger}(\theta) = w_R + \theta(\Delta G^0 + w_P - w_R) + \theta(1-\theta)(E_{rs} + E_{r\kappa}) \quad \text{(A1)}$$

where θ is the chemical transfer coefficient introduced in eqs 7 and 8. With focus on ionic strength effects, $G^{\ddagger}$ can be recast as

$$G^{\ddagger} = G^{\ddagger}(\theta) = w_R^s + w_R^{\kappa}(z_D, z_A) + \theta\Delta G_s^0 + \theta(1-\theta)E_{rs} + G_{\kappa}(z_D+\theta, z_A-\theta) - G_{\kappa}(z_D,z_A) \quad \text{(A2)}$$

The ionic strength dependence appears explicitly in $w_R = w_R^{\kappa}(z_D,z_A)$ and in the last two terms on the right-hand side of eq A2. ΔG_s^0 and w_R^s are the driving force and reactant work term at zero ionic strength. The ionic strength dependence is indicated by the superscript κ and by the dependence of the energy terms on z_De and z_Ae. $G_{\kappa}(z_D+\theta,z_A-\theta)$ is the electrostatic free energy of interaction between the donor and acceptor in the transition state. $G_{\kappa}(z_D,z_A)$ similarly represents this interaction in the reactants' equilibrium state. By the particular form of eq A2, the pure solvent and the ionic strength effects have been separated.

The merits of eq A2 can be illustrated by the following consideration. There is a certain electrostatic interaction free energy between the donor and acceptor molecules and the ionic atmosphere. In the reactants' equilibrium state, the interaction is determined by the *actual* donor and acceptor charges z_D and z_A. Nuclear and electrostatic *nonequilibrium* configurations, however, prevail in the transition state. These can be *formally* characterized by *equilibrium* interactions in which the real charges z_De and z_Ae have been replaced by $(z_D+\theta)e$ and $(z_A-\theta)e$ ($0<\theta<1$), respectively. $\theta \to 0$ if little ionic strength reorganization is needed prior to ET, as for strongly exergonic processes, whereas $\theta \to 1$ if most reorganization occurs prior to formation of the transition state, as for strongly endergonic processes. In ergoneutral ranges, $|\Delta G^0| \ll E_{rs}$, and $\theta \approx 0.5$. By using eq A2, we can thus exploit the equilibrium *forms* of the ionic interactions with the ionic atmosphere. In the following, we focus on the Debye−Hückel form, but we could also have dealt with the mean spherical approximation[14,37] or other more detailed but still analytical statistical mechanical forms.[37] This attractive option is a result of the particular form of eq A2.

The Debye−Hückel potential, associated with an ion of charge z_Se and radius a_S (S = D, A) at the distance r from the ion is[38]

$$\psi_D(r) = \frac{z_Se}{\epsilon_s r}\left\{\frac{\exp[\kappa(a_S - r)]}{1+\kappa a_S} - 1\right\} \quad \text{(A3)}$$

where κ is the inverse Debye length, eq 3. Insertion of eq A3 into eq A2 gives the following expression for the dynamic ionic strength dependent part of the activation free energy

$$G_{\kappa}(z_D+\theta,z_A-\theta) - G_{\kappa}(z_D,z_A) = \frac{\theta(1-\theta)e^2}{2\epsilon_s R}\left\{\frac{\exp[\kappa(a_D-R)]}{1+\kappa a_D} + \frac{\exp[\kappa(a_A-R)]}{1+\kappa a_A} - 2\right\} + \frac{\kappa e^2}{2\epsilon_s}\left[\frac{\theta(\theta+2z_D)}{1+\kappa a_D} + \frac{\theta(\theta-2z_A)}{1+\kappa a_A}\right] \quad \text{(A4)}$$

In turn, the following *interpolation formula*, eq A5/eq 13, applies to the ionic strength dependent part of the work term, w_R^{κ}

$$w_R^{\kappa} = \frac{z_Dz_Ae^2}{2\epsilon_s R}\left\{\frac{\exp[\kappa(a_D-R)]}{1+\kappa a_D} + \frac{\exp[\kappa(a_A-R)]}{1+\kappa a_A} - 2\right\} \quad \text{(A5)}$$

with a similar form for w_P^{κ} in which z_D has been replaced by $z_D + 1$ and z_A by $z_A - 1$. The factor "2" appears in the denominators of eqs A4 and A5, since these expressions refer to *self-energy* differences between the transition and reactant states, and between the reactants at distance R and infinite separation, respectively. Equation A5 has frequently been used as the sole basis for data analysis in ET processes.[1−6] This form was, however, originally introduced in a different context.[11] It constitutes a cruder approximation than Debye−Hückel theory itself and bears the character of interpolation between the ionic radii a_D and a_A.

The activation free energy terms in eq 11 can then be organized as in eq 7, with

$$\Delta G_{\kappa}^0 = \Delta G_{\kappa}^{00} + w_P^{\kappa} - w_R^{\kappa} \quad \text{(A6)}$$

$$\Delta G_{\kappa}^{00} = -\frac{\kappa e^2}{2\epsilon_s}\left[\frac{2z_D+1}{1+\kappa a_D} - \frac{2z_A-1}{1+\kappa a_A}\right] \quad \text{(A7)}$$

$$w_P^{\kappa} - w_R^{\kappa} = \frac{(z_D+1)(z_A-1) - z_Dz_A}{\epsilon_s R}e^2\left\{\frac{\exp[\kappa(a-R)]}{1+\kappa a} - 1\right\} \quad \text{(A8)}$$

where $2a \approx a_D + a_A$. Further, from eq A4

$$E_{r\kappa} = \frac{\kappa e^2}{2\epsilon_s}\left[\frac{1}{1+\kappa a_D} + \frac{1}{1+\kappa a_A}\right] + \frac{e^2}{2\epsilon_s R}\left\{\frac{\exp[\kappa(a_D - R)]}{1+\kappa a_D} + \frac{\exp[\kappa(a_A - R)]}{1+\kappa a_A} - 2\right\} \quad \text{(A9)}$$

Equations A5−A9 combined with eq 8 contain all the information about static and dynamic ionic strength effects. We point out the following:

(A) Ionic strength effects on w_R^κ dominate entirely for high charges or strongly exergonic processes where $\theta \rightarrow 0$.

(B) There are *two* ionic strength effects in the driving force and the reorganization free energy. One effect on the former is on the intrinsic $\Delta G°$ and given by eq A7, while the other one originates from the $w_P - w_R$ "correction". The ionic strength effect on the reorganization free energy is given by eq A9. The first term represents reorganization of the ionic atmosphere around each reactant molecule caused by the field change (ET) of the same ion, and the second term the reorganization around a given reactant molecule caused by the field change from the second reactant molecule.

(C) Only the ionic strength effects on w_R^κ and ΔG_κ^0 depend on the reactant charges, while $E_{r\kappa}$ is determined by the charge *transferred* (usually a single electronic charge).

A2. Partially Diffusion-Controlled Bimolecular ET. The steady state, partially diffusion-controlled bimolecular rate constant between two electrically *neutral* reactant molecules is[33]

$$k_{obs}^{(2)} = \frac{k_{ET}^{(1)0}\vec{k}_{diff}^{(2)0}}{k_{ET}^{(1)0} + \overleftarrow{k}_{diff}^{(1)0}} \quad \text{(A10)}$$

where $\vec{k}_{diff}^{(2)0}$ is the rate constant for intermolecular diffusion from infinite separation to the distance R where ET occurs. $\overleftarrow{k}_{diff}^{(1)0} = 1/\Delta V \vec{k}_{diff}^{(2)0}$ is the rate constant for diffusion in the opposite direction, and $k_{ET}^{(1)0}$ the unimolecular ET rate constant at the distance R.

The observed rate constant for ET between electrostatically *charged* reactant molecules is

$$k_{obs}^{(2)} = \frac{\vec{k}_{ET}^{(1)0}\,\vec{k}_{diff}^{(2)0}}{\vec{k}_{ET}^{(1)0} f + g\overleftarrow{k}_{diff}^{(1)0}} \quad \text{(A11)}$$

The quantities f and g are

$$f = R\int_R^\infty \exp\left[\frac{w_R(r)}{k_B T}\right]\frac{dr}{r^2} \qquad g = \exp\left(\frac{w_R}{k_B T}\right) \quad \text{(A12)}$$

where w_R is the work term. Equation A12 can be recast in the following form when the intermolecular interaction is Coulombic and screened solely by the solvent

$$k_{obs}^{(2)} = \frac{k_{ET}^{(1)0}\,\vec{k}_{diff}^{(2)}}{k_{ET}^{(1)0} + \overleftarrow{k}_{diff}^{(1)}} \quad \text{(A13)}$$

where $\vec{k}_{diff}^{(2)}$ and $\overleftarrow{k}_{diff}^{(1)}$ are given by

$$\vec{k}_{diff}^{(2)} = \vec{k}_{diff}^{(2)0}\frac{w_R}{k_B T}\frac{1}{\left[\exp\left(\frac{w_R}{k_B T}\right) - 1\right]} \qquad w_R = z_D z_A/\epsilon_s R \quad \text{(A14)}$$

$$\frac{\vec{k}_{diff}^{(2)}}{\overleftarrow{k}_{diff}^{(1)}} = K \qquad K = \Delta V \exp\left(-\frac{w_R}{k_B T}\right) \quad \text{(A15)}$$

K (volume mol^{-1}) is the "equilibrium constant" for formation of the "collision complex". The appropriate volume scale is the volume of the reaction zone where ET can occur. The space integration (see eq A12) is less straightforward when w_R incorporates screening by both the solvent and the ionic atmosphere.[33] We shall still use eqs A13 and A14, with $w_R = w_R^s + w_R\kappa$, cf. eq 11, which then, however, only apply approximately.

Another form of eq A13 is convenient for evaluation of the ionic strength effect, eq A16

$$k_{obs}^{(2)} = \frac{k_{ET}^{(2)}\vec{k}_{diff}^{(2)}}{k_{ET}^{(2)} + \vec{k}_{diff}^{(2)}} \quad \text{(A16)}$$

where $k_{ET}^{(2)}$ is the bimolecular ET rate constant in eq 4. This equation follows from eqs A10 and A15; it includes charge and ionic strength effects in both $k_{ET}^{(2)}$ and $\vec{k}_{diff}^{(2)}$, represented by eqs 4−6, 9−13, and A14.

Acknowledgment. We thank D. M. Kurtz, Jr., and M. K. Eidsness for protein samples and helpful discussions, and I. J. Dmochowski for the *p*-MDMA sample. T.J.J. thanks A. Tezcan for assistance with the laser spectroscopic measurements. This work was supported by the Technical University of Denmark, the Danish Technical Science Research Council, the National Institutes of Health (DK19038, Beckman Institute), and the Russian Foundation for Basic Research (A. N. Frumkin Institute).

References and Notes

(1) Wherland, S.; Gray, H. B. *Proc. Natl. Acad. Sci. U.S.A.* **1976**, *73*, 2950−2954.
(2) Wherland, S.; Gray, H. B. In *Biological Aspects of Inorganic Chemistry*, Addison, A. W., Cullen, W. R., Dolphin, D., James, B. R., Eds.; Wiley-Interscience: New York, 1977; pp 289−368.
(3) McArdle, J. V.; Gray, H. B.; Creutz, C.; Sutin, N. *J. Am. Chem. Soc.* **1974**, *96*, 5737−5741.
(4) Simondsen, R.; Tollin, G. *Biochemistry* **1983**, *22*, 3008−3016.
(5) Tollin, G.; Meyer, T. E.; Cusanovich, M. A. *Biochim. Biophys. Acta* **1986**, *853*, 29−41.
(6) Navarro, J. A.; De la Rosa, M. A.; Tollin, G. *Eur. J. Biochem.* **1991**, *199*, 239−243.
(7) Andersen, N. H.; Hervás, M.; Navarro, J. A.; De la Rosa, M. A.; Ulstrup, J. *Inorg. Chim. Acta* **1998**, *272*, 109−114.
(8) Brønsted, J. N. *Z. Phys. Chem.* **1922**, *102*, 169−207.
(9) Bjerrum, N. *Z. Phys. Chem.* **1924**, *108*, 82−100.
(10) Christiansen, J. A. *Z. Phys. Chem.* **1924**, *113*, 35−52.
(11) Debye, P. *Trans. Electrochem. Soc.* **1942**, *82*, 265−272.
(12) Watkins, J. A.; Cusanovich, M. A.; Meyer, T. E.; Tollin, G. *Protein Sci.* **1994**, *5*, 2104−2114.
(13) Dogonadze, R. R.; Kuznetsov, A. M. *J. Electroanal. Chem.* **1975**, *65*, 545−554.
(14) Waisman, E.; Worry, G.; Marcus, R. A. *J. Electroanal. Chem.* **1977**, *82*, 9−28.
(15) German, E. D.; Kuznetsov, A. M. *Elektrokhimiya* **1987**, *23*, 1671−1675.
(16) Lovenberg, W.; Walker, M. N. *Methods Enzymol.* **1978**, *53*, 340−346.
(17) Nakamura, A.; Ueyama, N. *Adv. Inorg. Chem.* **1991**, *33*, 39−67.
(18) Bertini, I.; Kurtz, D. M., Jr.; Eidsness, M. K.; Liu, G.; Luchinat, C.; Rosato, A.; Scott, R. A. *JBIC* **1998**, *3*, 401−410.
(19) Eidsness, M. K.; Ricie, K. A.; Burden, A. E.; Kurtz, D. M., Jr.; Scott, R. A. *Biochemistry* **1997**, *36*, 10406−10413.
(20) Jacks, C. A.; Bennett, L. E.; Raymond, W. N.; Lovenberg, W. *Proc. Natl. Acad. Sci. U.S.A.* **1974**, *71*, 1118−1122.
(21) Im, S.-C.; Sykes, A. G. *J. Chem. Soc., Dalton Trans.* **1996**, 2219−2222.

(22) Im, S.-C.; Zhuang-Jackson, H.-Y.; Kohsuma, T.; Kyritsis, P.; McFarlane, W.; Sykes, A. G. *J. Chem. Soc., Dalton Trans.* **1996**, 4287−4294.
(23) Przysiecki, C. T.; Bhattacharyya, A. K.; Tollin, G.; Cusanovich, M. A. *J. Biol. Chem.* **1985**, *260*, 1452−1456.
(24) Sekia, M.; Tomime, M.; Leonard, N. J. *J. Org. Chem.* **1967**, *33*, 318−322.
(25) Lovenberg, W.; Stobel, B. E. *Proc. Natl. Acad. Sci. U.S.A.* **1965**, *54*, 193−199.
(26) Sassoon, R. E.; Gershuni, S.; Rabani, J. *J. Phys. Chem.* **1992**, *96*, 4692−4698.
(27) Sutin, N.; Creutz, C. *Adv. Chem. Ser.* **1978**, *168*, 1−27.
(28) Stowell, M. H. B.; Larsen, R. W.; Winkler, J. R.; Rees, D. C.; Chan, S. I. *J. Phys. Chem.* **1993**, *97*, 3054−3057.
(29) Marcus, R. A.; Sutin, N. *Biochim. Biophys. Acta* **1985**, *811*, 265−322.
(30) Kuznetsov, A. M.; Ulstrup, J. *Electron Transfer in Chemistry and Biology. An Introduction to the Theory*; Wiley: Chichester, U.K., 1999.
(31) Brønsted, J. N. *Chem. Rev.* **1932**, *3*, 231−338.
(32) Marcus, R. A. *J. Phys. Chem. B* **1998**, *102*, 10071−10077.
(33) Schurr, J. M. *Biophys. J.* **1970**, *10*, 700−716.
(34) Hodges, H. L.; Holwerda, R. A.; Gray, H. B. *J. Am. Chem. Soc.* **1974**, *96*, 3132−3137.
(35) Iversen, G.; Kharkats, Y. I.; Ulstrup, J. *Mol. Phys.* **1998**, *94*, 297−306.
(36) Honig, B.; Nicholls, A. *Science* **1995**, *268*, 1144−1149.
(37) Wolynes, P. *J. Chem. Phys.* **1987**, *86*, 5133−5136.
(38) Debye, P.; Hückel, E. *Phys. Z.* **1923**, *24*, 186−206.